

# Multicarrier Access and Routing for Wireless Networking

**Diakoumis Gerakoulis**

*General Dynamics Advanced Information Systems, Bloomington, MN 55431, USA*  
*Email: diakoumis.gerakoulis@gd-ais.com*

*Received 28 February 2005; Recommended for Publication by Fary Z. Ghassemlooy*

A multicarrier access and routing system has been proposed for use in wireless networks. Users within each cell access a radio port (RP). All RPs are connected to a radio exchange node (REN) which routes the calls or packets. The uplink access is orthogonal multicarrier code-division multiple access (MC-CDMA) and the downlink transmission is multicarrier orthogonal code-division multiplexing (MC-OCDM). The REN contains a switch module which provides continuous routes between wireless terminals without demodulation/remodulation or channel decoding/reencoding. The switch module is nonblocking and has complexity and speed linearly proportional to its size. Also, the switch module does not introduce interference into the network. Any existing interference or noise in its input port is transferred to its output port. The input-output switch connections are assigned on demand by a control unit. A random input/output port assignment process can achieve maximum switch throughput.

**Keywords and phrases:** multicarrier access, multicarrier routing, multicarrier CDMA, radio exchange node, switch module.

## 1. INTRODUCTION

Multicarrier transmission methods have been widely accepted and used because of their advantages over single-carrier transmission in broadband wireless links. The existing multicarrier systems however, such as the orthogonal frequency-division multiplexing (OFDM), are only defined for the physical layer, while wireless networks also require a method for multiuser access and routing. This paper focuses on the development of a multicarrier system that operates at physical, multiple access and routing level. The transmission and access is based on orthogonal multicarrier (MC) code-division multiple access (CDMA), see [1, 2, 3, 4, 5]; while the routing scheme on code-division multiplexing [6].

The wireless network is assumed to have the configuration shown in Figure 1. It consists of a radio exchange node (REN) connected to a number of radio ports (RPs). All RPs are connected to the radio exchange node (REN) which routes packets or calls between RPs. Users within each cell access the corresponding radio port (RP) by an orthogonal multicarrier CDMA described in [5]. All uplink transmissions require synchronization. The downlink transmission is multicarrier orthogonal code-division multiplexing (OCDM) described in [4]. The REN contains the

switch module which routes packets and calls between radio ports without demodulation/remodulation or channel decoding/reencoding. Such a wireless network then provides a continuous mobile-to-mobile route that achieves high network throughput and spectral efficiency.

In Section 2 we present the system description and verify its functional correctness. In Section 3 we examine the network capacity and performance which includes the routing capacity and the network interference.

## 2. SYSTEM DESCRIPTION

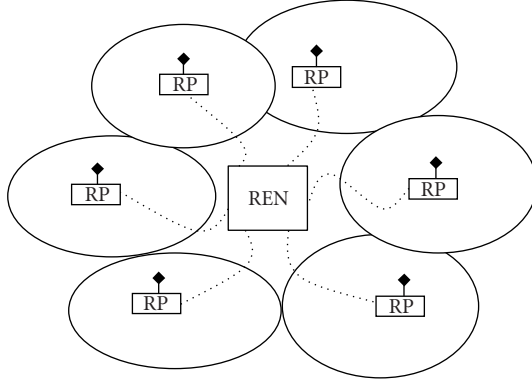
The wireless access and routing system is shown in Figure 2. Wireless terminals within each cell access the corresponding radio port by orthogonal multicarrier code-division multiple access (MC-CDMA) [5]. The uplink transmission and reception is described below, in Section 2.1. The received signal at the REN is routed by the switch module to the destination output port. The source-destination information is supplied by the control unit. The switch module is an  $M$ -input,  $M$ -output, nonblocking, routing fabric which is described in Section 2.2. The output port signal is transmitted in the downlink and received by the wireless terminal as described in Section 2.3.

### 2.1. The uplink

The transmitter of wireless terminal  $\ell$  in microcell  $m$  is shown in Figure 3. The input data stream  $x^{(\ell,m)}$  of rate  $R$  is

---

This is an open access article distributed under the Creative Commons Attribution License, which permits unrestricted use, distribution, and reproduction in any medium, provided the original work is properly cited.



RP: radio port  
REN: radio exchange node

FIGURE 1: The wireless access and routing network.

spread by the Hadamard sequence  $w_\ell$  with rate  $LR$ . Assuming that  $x^{(\ell,m)}$  represents a complex-valued signaling point, that is,  $x^{(\ell,m)} = \alpha^{(\ell,m)} + j\beta^{(\ell,m)}$ , the spread signal is

$$\begin{aligned}\bar{Y}_k^{(\ell,m)} &= x^{(\ell,m)} w_{\ell,k} \\ &= \alpha^{(\ell,m)} w_{\ell,k} + j\beta^{(\ell,m)} w_{\ell,k} \quad \text{for } k = 0, 1, \dots, L-1.\end{aligned}\quad (1)$$

The spread signal  $\bar{Y}_k^{(\ell,m)}$  is also encoded (multiplied) with pseudorandom noise (PN) sequence  $\mathbf{g}_m = [g_{m,k}]$  in order to suppress interference from other uplink microcells with the same carrier frequency.  $\mathbf{g}_m$  is the same for all uplink transmissions in microcell  $m$ , has the same rate ( $LR$ ) as the sequence  $w_\ell$ , and thus  $\mathbf{g}_m$  does not spread the signal further. The resulting signal  $Y_k^{(\ell,m)} = \bar{Y}_k^{(\ell,m)} g_{m,k}$  is then encoded by a multicarrier encoder which in this case is an orthogonal frequency-division multiplexor (OFDM) having  $L$  subcarriers. The  $L$  parallel points  $Y_k^{(\ell,m)}$  then enter an IFFT given by

$$y_n^{(\ell,m)} = \frac{1}{L} \sum_{k=0}^{L-1} Y_k^{(\ell,m)} e^{j2\pi(kn/L)}. \quad (2)$$

The parallel outputs  $y_n^{(\ell,m)}$  for  $n = 0, 1, \dots, L-1$  then enter a P/S converter where a guard time or cyclic prefix is added. The P/S converter output  $s^{(\ell,m)}(n)$  is converted into an analog signal  $s^{(\ell,m)}(t)$  which is up-converted into the uplink carrier  $f_u^{(m)}$  and then transmitted to the radio port (RP). At the REN the received signal at input port  $m$  is given by

$$r_u^{(m)}(t) = \sum_{\ell=0}^{L-1} r_u^{(\ell,m)}(t) = \sum_{\ell=0}^{L-1} [h_u^{(\ell,m)}(t) * s_u^{(\ell,m)}(t)], \quad (3)$$

where  $r_u^{(\ell,m)}(t)$  is the received uplink signal from terminal  $\ell$  in microcell  $m$ ,  $h_u^{(\ell,m)}(t)$  is the impulse response of the corresponding uplink channel, and  $(*)$  denotes convolution (the channel is assumed noiseless at the moment). The analog signal  $r_u^{(m)}(t)$  enters the uplink receiver (or recovery

circuit) shown in Figure 4, where is down-converted to base-band, digitized into signal  $z_u^{(m)}(n)$ , and then decoded by the a MC-decoder (i.e., an OFDM-decoder). In the OFDM-decoder  $z_u^{(m)}(n)$  is S/P converted into  $L$  parallel data points  $z_{u;n}^{(m)}$  for  $n = 0, 1, \dots, L-1$ , which enter an FFT given by

$$\bar{Z}_{u;k}^{(m)} = \sum_{n=0}^{L-1} z_{u;n}^{(m)} e^{-j2\pi(kn/L)} \quad \text{for } k = 0, 1, \dots, L-1. \quad (4)$$

The post-FFT signal is given by

$$\begin{aligned}\bar{Z}_{u;k}^{(m)} &= \sum_{\ell=1}^L H_{u;k}^{(\ell,m)} \bar{Y}_k^{(\ell,m)} \\ &= g_{m,k} \sum_{\ell=1}^L H_{u;k}^{(\ell,m)} x^{(\ell,m)} w_{\ell,k} \quad \text{for } k = 0, 1, \dots, L-1,\end{aligned}\quad (5)$$

where  $H_{u;k}^{(\ell,m)}$  is the uplink channel transfer function (CTF) of user  $\ell$  in microcell  $m$  at subcarrier  $k$ . In the above we have used the assumption of perfect synchronization between transmitting signals in order to verify the functional correctness of the process. The  $L$  parallel  $\bar{Z}_k^{(m)}$  points then enter a P/S converter, the output of which is first despread by  $g_{m,k}$  to provide the signal

$$Z_{u;k}^{(m)} = \sum_{\ell=1}^L H_{u;k}^{(\ell,m)} x^{(\ell,m)} w_{\ell,k} \quad \text{for } k = 0, 1, \dots, L-1. \quad (6)$$

The signal  $Z_{u;k}^{(m)}$  is then despread by the  $L$  Hadamard sequences  $w_\ell = [w_{\ell,0}, w_{\ell,2}, \dots, w_{\ell,L-1}]$  in parallel in order to recover the data of each uplink transmission in microcell  $m$ . In particular, the output signal of despreader-1 is given by

$$\begin{aligned}\sum_{k=0}^{L-1} Z_{u;k}^{(m)} w_{1,k} &= \sum_{k=0}^{L-1} \left[ \sum_{\ell=1}^L H_{u;k}^{(\ell,m)} X_k^{(\ell,m)} \right] w_{1,k} \\ &= \sum_{k=0}^{L-1} \sum_{\ell=1}^L (H_{u;k}^{(\ell,m)} x^{(\ell,m)} w_{\ell,k}) w_{1,k} \\ &= \sum_{\ell=1}^L H_u^{(\ell,m)} x^{(\ell,m)} \sum_{k=0}^{L-1} w_{\ell,k} w_{1,k} \\ &= \begin{cases} LH_u^{(1,m)} x^{(1,m)} & \text{for } \ell = 1, \\ 0 & \text{for } \ell \neq 1. \end{cases}\end{aligned}\quad (7)$$

In the above we have made the assumption of frequency-flat channel, that is,  $H_{u;k}^{(\ell,m)} = H_u^{(\ell,m)}$  for all  $k$ .

## 2.2. The switch module

Let  $G_u^{(\ell,m)}$  denote the recovered signal of user  $\ell$  at input port  $m$ ; then

$$G_u^{(\ell,m)} = LH_u^{(\ell,m)} x^{(\ell,m)}. \quad (8)$$

There are  $L$  such signals at the output of the uplink recovery

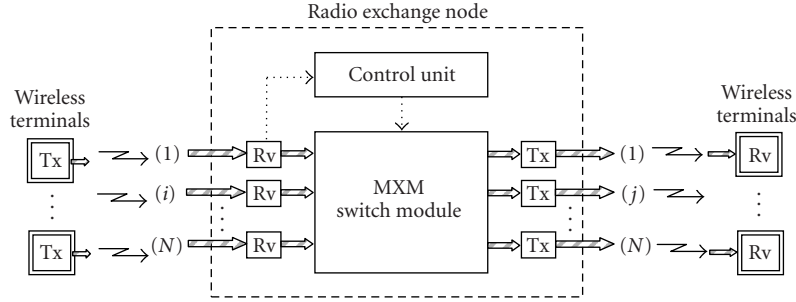


FIGURE 2: The wireless access and routing system.

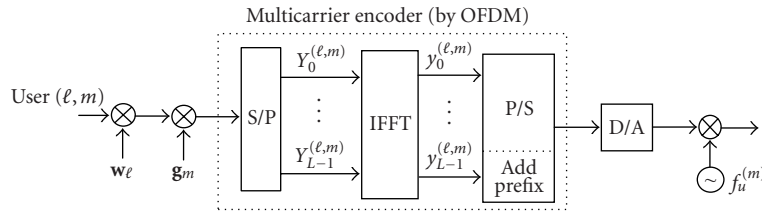
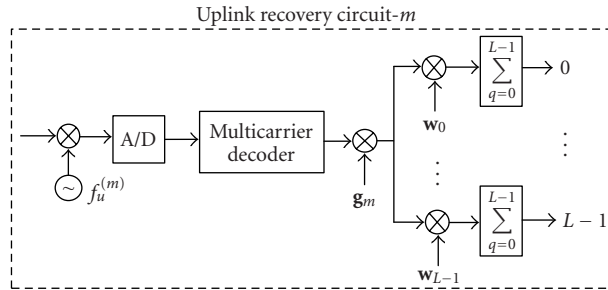


FIGURE 3: The wireless terminal transmitter.


 FIGURE 4: The uplink receiver (uplink recovery circuit- $m$ ).

circuit- $m$  where each signal is then encoded by its corresponding destination encoder- $(\ell, m)$ , shown in Figure 5. Let the destination of channel  $\ell$  at input port  $m$  be the output port  $m'$  and channel  $\ell'$ , then the function of destination encoder  $(\ell, m)$  is denoted as  $(\ell, m) \rightarrow (\ell', m')$  for  $\ell, \ell' = 0, 1, \dots, L-1$  and  $m, m' = 0, 1, \dots, M-1$ , where  $M$  is the number of input or output ports of the switch module and  $L$  the number of channels per input or output port.

The signal at the output of the destination encoder- $(\ell, m)$  then is  $G_u^{(\ell, m)} \mathbf{w}_{\ell'} \mathbf{w}_{m'}$ , where  $\mathbf{w}_{\ell'} = [w_{\ell', k}]$  and  $\mathbf{w}_{m'} = [w_{m', n}]$  are the destination channel and destination port orthogonal sequences, respectively. If the rate of  $G_u^{(\ell, m)}$  is  $R$ , then the rate of the destination channel spread signal  $G_u^{(\ell, m)} \mathbf{w}_{\ell'}$  is  $R_L = LR$  and the rate of the destination channel and port spread signal  $G_u^{(\ell, m)} \mathbf{w}_{\ell'} \mathbf{w}_{m'}$  is  $R_M = LR_L = LMR$ . Hence,  $T = LT_c = LMT_{cc}$ , where  $T$  is the symbol length,  $T_c$  is the chip length of sequence  $\mathbf{w}_{\ell'}$ , and  $T_{cc}$  is the chip length of sequence  $\mathbf{w}_{m'}$ .

The signals at the outputs of the destination encoders are then summed up over all channels in each port and over all

ports to provide the signal

$$G_{k,n} = \sum_{m'=0}^{M-1} \sum_{\ell'=0}^{L-1} G_u^{(\ell, m)} w_{\ell', k} w_{m', n}. \quad (9)$$

Each destination port  $m'$  then recovers its corresponding channels from the signal  $G_{k,n}$  (taking it from the switch bus) by using the port decoder (shown in Figure 5), which despreads  $G_{k,n}$  with the port destination sequence  $\mathbf{w}_{m'}$ . The output of the port decoder-1 is then given by

$$\begin{aligned} G_{d;k}^{(m'=1)} &= \sum_{n=0}^{M-1} G_{k,n} w_{m'=1, n} \\ &= \sum_{m'=0}^{M-1} \sum_{\ell'=0}^{L-1} G_u^{(\ell, m)} w_{\ell', k} \sum_{n=0}^{M-1} w_{m', n} w_{1, n} \\ &= \sum_{\ell'=0}^{L-1} G_u^{(\ell', 1)} w_{\ell', k}. \end{aligned} \quad (10)$$

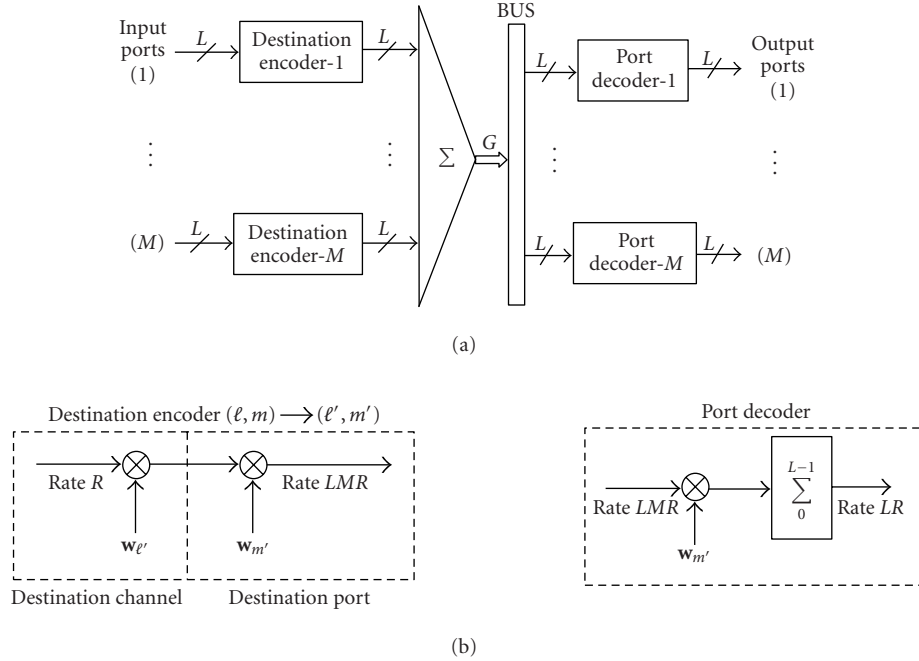


FIGURE 5: The switch module.

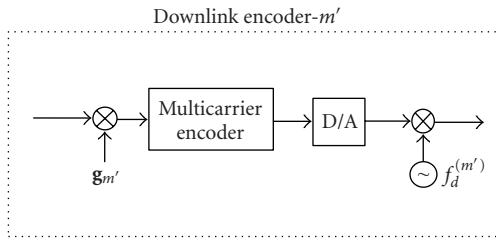


FIGURE 6: The downlink transmitter (downlink encoder).

Hence, the signal at the output of port decoder- $m'$  (output port- $m'$ ) is given by

$$\bar{G}_{d;k}^{(m')} = \sum_{\ell'=0}^{L-1} G_u^{(\ell',m')} w_{\ell',k}. \quad (11)$$

The above indicates that each output port is a sum of up to  $L$  channels which may originate in different input ports.

### 2.3. The downlink

The signal  $\bar{G}_{d;k}^{(m')}$  then enters the downlink transmitter (or downlink encoder) shown in Figure 6, where it is encoded (multiplied) with the PN-sequence  $\mathbf{g}_{m'} = [g_{m',k}]$  of the downlink microcell- $m'$  to provide the signal

$$G_{d;k}^{(m')} = \mathbf{g}_{m',k} \bar{G}_{d;k}^{(m')} = \mathbf{g}_{m',k} \sum_{\ell'=0}^{L-1} G_u^{(\ell',m')} w_{\ell',k}. \quad (12)$$

Then,  $G_{d;k}^{(m')}$  is encoded by a MC-encoder  $m'$  (i.e., an OFDM encoder) by taking its IFFT:

$$y_n^{(m')} = \frac{1}{L} \sum_{k=0}^{L-1} G_{d;k}^{(m')} e^{j2\pi(kn/L)} \quad \text{for } n = 0, 1, \dots, L-1. \quad (13)$$

After the P/S converter, the digital signal  $y^{(m')}(n)$  is converted into an analog signal  $s^{(m')}(t)$  which is then up-converted to the downlink carrier of microcell  $m'$ ,  $f_d^{(m')}$ . The receiver of wireless terminal  $\ell'$  in microcell  $m'$  is shown in Figure 7. The received downlink signal from the REN is given by

$$r_d^{(m')}(t) = \sum_{\ell'=0}^{L-1} r_d^{(\ell',m')}(t) = h_d^{(m')}(t) * s_d^{(m')}(t), \quad (14)$$

where  $s_d^{(m')}(t)$  is the sum of all downlink signals  $\ell'$ , that is,  $s_d^{(m')}(t) = \sum_{\ell'=0}^{L-1} s_d^{(\ell',m')}(t)$ , and  $s_d^{(\ell',m')}(t)$  is the downlink signal of a terminal  $\ell'$ .  $s_d^{(\ell',m')}(t)$  are orthogonal to each other. Also,  $h_d^{(m')}(t)$  is the impulse response of the downlink channel in microcell  $m'$ . The received signal  $r_d^{(m')}(t)$  is down-converted to baseband and then an A/D converter provides the digital signal  $r_d^{(m')}(n)$  which enters the OFDM decoder. At the decoder after the cyclic prefix is removed, an S/P converter provides  $L$  parallel data points  $z_{d;n}^{(m')}$ . The  $L$  parallel points  $z_{d;n}^{(m')}$ , for  $n = 0, 1, \dots, L-1$ , then enter an FFT which provides the signal

$$\bar{Z}_{d;k}^{(m')} = \sum_{n=0}^{L-1} z_{d;n}^{(m')} e^{-j2\pi(kn/L)} \quad \text{for } k = 0, 1, \dots, L-1. \quad (15)$$

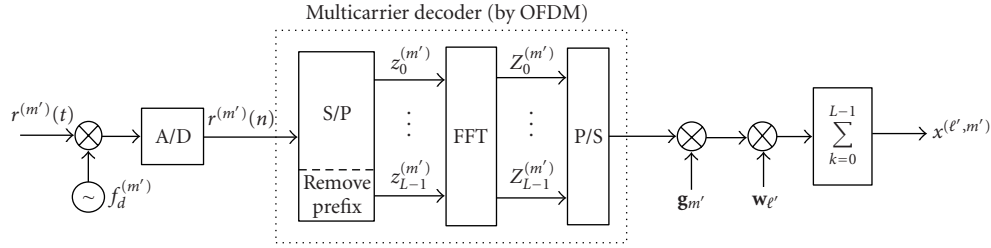


FIGURE 7: The wireless terminal receiver.

The post-FFT signal  $\bar{Z}_{d;k}^{(m')}$  is given by

$$\begin{aligned} \bar{Z}_{d;k}^{(m')} &= H_{d;k}^{(m')} G_{d;k}^{(m')} = H_{d;k}^{(m')} g_{m',k} \sum_{\ell'=0}^{L-1} G_u^{(\ell',m')} w_{\ell',k} \\ &= H_{d;k}^{(m')} g_{m',k} L \sum_{\ell'=0}^{L-1} H_u^{(\ell',m')} x^{(\ell',m')} w_{\ell',k}, \end{aligned} \quad (16)$$

where  $H_{d;k}^{(m')}$  is the transfer function of the downlink channel in microcell  $m'$  at subcarrier  $k$  and  $H_u^{(\ell',m')}$  is the transfer function of the uplink channel of terminal  $\ell'$  in microcell  $m'$ , (which has been assumed to be constant at all subcarriers). In the above we have used (8) and (12).  $\bar{Z}_{d;k}^{(m')}$  is then despread with the PN-sequence  $g_{m',k}$  to provide the signal

$$Z_{d;k}^{(m')} = L H_{d;k}^{(m')} \sum_{\ell'=0}^{L-1} H_u^{(\ell',m')} x^{(\ell',m')} w_{\ell',k}. \quad (17)$$

The desired signal of a wireless terminal  $\ell'$  is then recovered by despreading  $Z_{d;k}^{(m')}$  with the sequence  $w_{\ell'}$ , that is,

$$\begin{aligned} \sum_{k=0}^{L-1} Z_{d;k}^{(m')} w_{\ell',k} &= \sum_{k=0}^{L-1} \left[ L H_{d;k}^{(m')} \sum_{\ell'=0}^{L-1} H_u^{(\ell',m')} x^{(\ell',m')} w_{\ell',k} \right] w_{\ell',k} \\ &= \sum_{k=0}^{L-1} \sum_{\ell'=0}^{L-1} L H_{d;k}^{(m')} H_u^{(\ell',m')} x^{(\ell',m')} w_{\ell',k} w_{\ell',k} \\ &= \sum_{\ell'=0}^{L-1} L H_d^{(m')} H_u^{(\ell',m')} x^{(\ell',m')} \sum_{k=0}^{L-1} w_{\ell',k} w_{\ell',k} \\ &= \begin{cases} L^2 H_d^{(m')} H_u^{(\ell',m')} x^{(\ell',m')} & \text{for } \ell' = \ell', \\ 0 & \text{for } \ell' \neq \ell'. \end{cases} \end{aligned} \quad (18)$$

In the above we have made the assumption that the downlink channel in microcell  $m'$  is frequency flat, that is,  $H_{d;k}^{(m')} = H_d^{(m')}$  for all  $k$ . The purpose of the above analysis is to verify the functional correctness of the process and therefore it does not include the effects of noise or interference. The effects of interference and noise are examined in the performance section.

### 3. CAPACITY AND PERFORMANCE EVALUATION

#### 3.1. The routing capacity

We consider a switch module with  $M$  input and  $M$  output ports, and  $L$  access channels per port. The switch will then provide a *capacity* of  $ML \times ML$  simultaneous connections. This capacity is achieved when the REN is fully equipped. A fully equipped REN has  $M$  multicarrier uplink receivers (uplink recovery circuits) and  $M$  multicarrier downlink transmitters. The switch module has  $ML$  destination encoders in the input ( $L$  in each input) and  $L$  port decoders at the output ( $L$  in each output port). Therefore the required circuitry of the switch module is *linearly proportional* to the its size  $M$  (this may be compared to a crossbar switch that has  $M^2$  crosspoints). Given the above assumptions the switch fabric is *nonblocking* for any incoming call to an input port. That is, there is always a connection available to a destination output. The number of active calls at an input port  $i$  or output port  $j$  must be less than  $L$ , that is,  $\sum_{j=0}^M t_{ij} \leq L$  and  $\sum_{i=0}^M t_{ij} \leq L$ , where  $t_{ij}$  is the number of calls between  $i$  and  $j$ . A call may be blocked by the input- and/or output-port capacity limit  $L$ .

The input-output connections are assigned on demand by the control unit (CU). That is, the CU receives an input-output call request via a demand or control channel and makes the requested connection in the switch module which is used to route the call. The assignment input-output connection in the switch module by the CU is made upon availability (at random) without rearranging the on-going calls. This simple approach is shown to achieve maximum switch throughput for the type of code-multiplexed switch module presented here [6]. This is not the case in time-multiplexed switching which requires more complex routing control algorithms to achieve maximum throughput [7].

The speed or the clock rate of an  $M \times M$  switch module is  $M$  times the rate of the incoming signal. This is  $MLR$ ; where  $L$  is the number of access channels per port, and  $R$  is the symbol rate per access channel (when there is no demodulation, i.e., no phase detection and symbol recovery at the REN). If we consider demodulation of  $\mathcal{M}$ -ary symbols at the REN, the speed of the switch will increase by a factor  $\log_2 \mathcal{M}$  (i.e.,  $(\log_2 \mathcal{M})ML$ ).

#### 3.2. The network interference

Let  $n_{u;k}^{(m')}$  represent the sum of uplink multiple access

interference (MAI) and AWGN of cell  $m$  in frequency bin  $k$ , that is,

$$n_{u;k}^{(m)} = I_{u;k}^{(m)} + n_o, \quad (19)$$

where  $I_{u;k}^{(m)}$  represent the intercell interference. The intracell interference is zero if we assume all uplink transmissions are perfectly synchronized. The received uplink signal then is

$$Z_k^{(m)} = \sum_{\ell=0}^{L-1} H_u^{(\ell,m)} x^{(\ell,m)} w_{\ell,k} + n_{u;k}^{(m)}. \quad (20)$$

The signal at the output of the uplink recovery circuit then is

$$G_u^{(\ell,m)} = \frac{1}{L} \sum_{k=0}^{L-1} Z_k^{(m)} w_{\ell,k} = H_u^{(\ell,m)} x^{(\ell,m)} + N_u^{(m)}, \quad (21)$$

where

$$N_u^{(m)} = \frac{1}{L} \sum_{k=0}^{L-1} n_{u;k}^{(m)} w_{\ell,k} \quad \forall \ell. \quad (22)$$

The signal at the switch bus is

$$G_{k,n} = \sum_{m'=0}^{M-1} \sum_{\ell'=0}^{L-1} H_u^{(\ell',m')} x^{(\ell',m')} w_{\ell',k} w_{m',n} + N_{k,n}, \quad (23)$$

where

$$N_{k,n} = \sum_{m'=0}^{M-1} \sum_{\ell'=0}^{L-1} N_u^{(m')} w_{\ell',k} w_{m',n}. \quad (24)$$

The downlink signal at the output port  $m'$  in frequency bin  $k$  is given by

$$G_{d;k}^{(m')} = \sum_{\ell'=0}^{L-1} H_u^{(\ell',m')} x^{(\ell',m')} w_{\ell',k} + N_{u/d;k}^{(m')}, \quad (25)$$

where

$$N_{u/d;k}^{(m')} = \frac{1}{M} \sum_{n=0}^{M-1} N_{k,n} w_{m',n}. \quad (26)$$

The received downlink signal of cell  $m'$  in frequency bin  $k$  is

$$\begin{aligned} Z_{d;k}^{(m')} &= H_{d;k}^{(m')} G_{d;k}^{(m')} + n_{d;k}^{(m')} \\ &= H_{d;k}^{(m')} \left[ \sum_{\ell'=0}^{L-1} H_u^{(\ell',m')} x^{(\ell',m')} w_{\ell',k} + N_{u/d;k}^{(m')} \right] + n_{d;k}^{(m')}. \end{aligned} \quad (27)$$

The signal at the output of the wireless terminal receiver then is

$$\frac{1}{L} \sum_{k=0}^{L-1} Z_{d;k}^{(m')} w_{\ell',k} = H_d^{(m')} H_u^{(\ell,m)} x^{(\ell,m)} + N_{u/d}^{(m')} + N_d^{(m')}, \quad (28)$$

where

$$N_{u/d}^{(m')} = \frac{1}{L} \sum_{k=0}^{L-1} H_{d;k}^{(m')} N_{u/d;k}^{(m')} w_{\ell',k}, \quad N_d^{(m')} = \frac{1}{L} \sum_{k=0}^{L-1} n_{d;k}^{(m')} w_{\ell',k}. \quad (29)$$

Now, replacing  $n_{u;k}^{(m)} = I_{u;k}^{(m)} + n_o$  and  $n_{d;k}^{(m')} = I_{d;k}^{(m')} + n_o$ , ( $I_{d;k}^{(m')}$  is the downlink other-cell interference in frequency bin  $k$ ) and taking the variance of the total MAI plus noise in the downlink receiver, we have

$$\begin{aligned} \sigma_{N^{(m')}}^2 &= E \left[ \left| N_{I;u/d}^{(m')} + N_{I;d}^{(m')} + N_{n;u/d}^{(m')} + N_{n;d}^{(m')} \right|^2 \right] \\ &= E \left[ \left| N_{I;u/d}^{(m')} \right|^2 \right] + E \left[ \left| N_{I;d}^{(m')} \right|^2 \right] + 2E \left[ N_{I;u/d}^{(m')} N_{I;d}^{(m')} \right] \\ &\quad + 2E \left[ N_{I;u/d}^{(m')} N_{n;d}^{(m')} \right] + 2E \left[ N_{I;d}^{(m')} N_{n;u/d}^{(m')} \right] \\ &\quad + E \left[ \left| N_{n;u/d}^{(m')} \right|^2 \right] + E \left[ \left| N_{n;d}^{(m')} \right|^2 \right], \end{aligned} \quad (30)$$

where the term  $N_{I;x}^{(m')}$  is due to MAI and the term  $N_{n;x}^{(m')}$  is due to noise ( $x \rightarrow u/d$  or  $d$ ). As we observe the variance of the MAI and noise has the following terms (in the order they appear): the uplink (transferred;  $u/d$ ) MAI, the downlink MAI, the cross-product of the uplink MAI and the downlink MAI, the cross-product of the uplink MAI and the downlink noise, the cross-product of the uplink noise and the downlink MAI, the uplink noise, and the downlink noise. There are seven terms of interference and noise instead of the typical two terms (MAI and AWGN) in a single-hop point-to-point system.

In the above analysis we have assumed no demodulation at the REN, that is, no phase detection and symbol recovery and no channel decoding at the REN. If we had assumed demodulation, that is, making a hard decision after MC-decoding and before MC-reencoding, that is,  $x^{(\ell,m)} = \alpha^{(\ell,m)} + j\beta^{(\ell,m)} \rightarrow \{-1, 1\}$ , then that would effectively decouple the downlink from the uplink. In this case the interference transfer terms (cross-terms) will not appear. The speed of the switch however will increase by a factor  $\log_2 \mathcal{M}$  (i.e.,  $(\log_2 \mathcal{M})ML$ ). Therefore the cross-terms appear as a result of coupling between uplink and downlink in the case of no demodulation at the REN.

### 3.3. The signal amplitude distribution

Let  $x_i^{(\ell,m)} = \alpha_i^{(\ell,m)} + j\beta_i^{(\ell,m)}$  represents the  $i$ th  $\mathcal{M}$ -ary symbol of the  $\ell$ th user at the  $m$ th input port. Also, let  $\mathbf{w}_\ell(l)$  be the destination channel code in the destination encoder circuit, see Figure 5, having rate  $LR$  and chip duration  $T_c = 1/LR$ .

The signal amplitudes of the inphase (I) and quadrature (Q) components, respectively, are

$$a_i^{(m)} = \sum_{l=1}^L \alpha_i^{(\ell,m)} \mathbf{w}_\ell(l), \quad b_i^{(m)} = \sum_{l=1}^L \beta_i^{(\ell,m)} \mathbf{w}_\ell(l). \quad (31)$$

This signal will be overspread with the destination port code  $\mathbf{w}_m(k)$  at the rate  $LMR$  corresponding to chip duration  $T_{cc} = 1/LMR$ . The signal amplitudes of the (I) and (Q) components of the  $i$ th symbol then are, respectively,

$$A_i = \sum_{m=1}^M a_i^{(m)} \mathbf{w}_m(k), \quad B_i = \sum_{m=1}^M b_i^{(m)} \mathbf{w}_m(k), \quad (32)$$

where  $A_i$  and  $B_i$  represent (I) and (Q) components of the signal in the switch bus. Then, a port decoder will provide the signal of the output port  $m'$  by despreading it with the corresponding code  $\mathbf{w}_{m'}(n)$ , that is,  $\sum_{m'=1}^M A_i \mathbf{w}_{m'}(n) = \sum_{m'=1}^M \sum_{m=1}^M a_i^{(m)} \mathbf{w}_{m'}(n) \mathbf{w}_m(k) = \sum_{m'=1}^M a_i^{(m')} \delta_a(m, m')$ , where  $\delta_a(m, m') = \sum_{m=1}^M \mathbf{w}_{m'}(n) \mathbf{w}_m(k) = 1$  if  $m = m'$  and zero otherwise.

Therefore, assuming that the chip amplitude remains constant for duration  $T_c = 1/LR$ , the switch does not introduce any interference during the process of routing.

The amplitudes of the I and Q components of the  $i$ th  $\mathcal{M}$ -ary symbol of the  $n$ th user in the switch bus are, respectively,

$$S_I^{(n)}(i) = A_i^{(n)} + \bar{I}_I^{(n)}(i), \quad S_Q^{(n)}(i) = B_i^{(n)} + \bar{I}_Q^{(n)}(i). \quad (33)$$

The terms  $\bar{I}_I(i)$  and  $\bar{I}_Q(i)$  represent the interference from other users and AWGN during  $i$ th symbol. The mean of the interference terms is zero and the variance is  $\sigma_I^2 = \text{var}[\bar{I}_I(i)] = \text{var}[\bar{I}_Q(i)]$ .  $A_i^{(n)} = \cos \phi_i^{(n)}$  and  $B_i^{(n)} = \sin \phi_i^{(n)}$ , where  $\phi_i^{(n)}$  denotes the phase angle of the  $i$ th  $\mathcal{M}$ -ary symbol of the  $n$ th user signal, and they take values in the sets

$$\begin{aligned} A_i^{(n)} &\in \left\{ \cos \left[ \frac{(2j-1)\pi}{\mathcal{M}} \right], j = 1, 2, \dots, \mathcal{M} \right\}, \\ B_i^{(n)} &\in \left\{ \sin \left[ \frac{(2j-1)\pi}{\mathcal{M}} \right], j = 1, 2, \dots, \mathcal{M} \right\}. \end{aligned} \quad (34)$$

It is assumed that the sequences of phase angles  $\phi_i^{(n)}$  are independent and identically distributed (i.i.d.). That is, there is independence between the  $j$  symbols and between different  $n$  (user signals) and are also identically distributed. The distribution of the phase angle  $\phi_i^{(n)}$  is assumed to be uniform in the set  $\{\pi/\mathcal{M}, 3\pi/\mathcal{M}, \dots, (2M-1)\pi/\mathcal{M}\}$  and subsequently the phase components  $A_i^{(n)}$  and  $B_i^{(n)}$  are i.i.d. for different  $n$  and  $i$  and uniformly distributed with equal probability  $(1/\mathcal{M})$  in the above sets. For the same  $n$  and  $i$ ,  $A_i^{(n)}$  and  $B_i^{(n)}$  are not independent of each other but are uncorrelated, since  $E\{A_i^{(n)}\} = E\{B_i^{(n)}\} = 0$ ,  $E\{A_i^{(n)}B_i^{(n)}\} = 0$ , and

$E\{[A_i^{(n)}]^2\} = E\{[B_i^{(n)}]^2\} = 1/2$ . Provided that the switch size is sufficiently large ( $M \geq 8$ ), we can apply the central limit theorem (CLT) on each of the asymptotically Gaussian random variables  $S_I^{(n)}(i)$  or  $(S_Q^{(n)}(i))$ . Then the (unconditional) mean and variance are  $E\{S_I^{(n)}(i)\} = 0$  and  $\text{Var}\{S_I^{(n)}(i)\} = N(1 + \sigma_I^2)$ . The conditional mean is

$$E\{S_I^{(n)}(i) | A_i^{(n)}, n = 1, 2, \dots, ML\} = \sum_{k=1}^M \sum_{l=1}^L \alpha_i^{(\ell,m)} \mathbf{w}_\ell(l) \mathbf{w}_m(k). \quad (35)$$

The conditional variance is  $\text{Var}\{S_I^{(n)}(i) | A_i^{(n)}, n = 1, 2, \dots, ML\} = N\sigma_I^2$  (similarly for the Q component). Thus the dynamic amplitude range of the sum-signal in the switch bus when no interference is present is given by

$$[-MLK_j(\mathcal{M}), MLK_j(\mathcal{M})],$$

$$\text{for } j=I \quad K_I(\mathcal{M}) = \max_k \left\{ \cos \frac{(2k-1)\pi}{\mathcal{M}} \right\} = \cos \frac{\pi}{\mathcal{M}},$$

$$\text{for } j=Q \quad K_Q(\mathcal{M}) = \max_k \left\{ \sin \frac{(2k-1)\pi}{\mathcal{M}} \right\} = \sin \frac{(2k^*-1)\pi}{\mathcal{M}}, \quad (36)$$

where  $k^*$  is the integer part of  $[(\mathcal{M}/4) + (1/2)]$ . When interference is taken into account we must add multiples of the noise variance. For example,  $3\sqrt{ML}\sigma_I$ , for 99.74% confidence. That is,

$$[-MLK_j(\mathcal{M}) - 3\sqrt{ML}\sigma_I, MLK_j(\mathcal{M}) + 3\sqrt{ML}\sigma_I]. \quad (37)$$

The above dynamic range should be compared with the range  $[-1, 1]$  for bipolar samples for time-division multiplexed switch modules.

#### 4. CONCLUSION

We have presented a multicarrier access and routing system for wireless networking. Users within each cell access a radio port (RP). All RPs are connected to a radio exchange node (REN) which routes calls or packets to other cells in the network. The uplink transmission is an orthogonal multicarrier CDMA (all uplink transmissions require synchronization). The network provides continuous routes between wireless terminals without demodulation/remodulation or channel decoding/reencoding at the REN. The REN has a nonblocking switch module with hardware complexity and speed linearly proportional to its size. The switch module does not introduce interference into the network. Any existing interference or noise to its input ports will be transferred to its output (assuming no demodulation/remodulation at the switch). The total interference at the receiver of an end-to-end link is the sum of the interferences of the input link, the output link, and their cross-product. The distribution of the signal amplitude in an  $M \times M$  switch module is asymptotically Gaussian (for large  $M$ ) with zero mean and variance proportional to  $M$ , while its dynamic range is

$[-MLK_j, MLK_j]$ ; where  $K_j$  is the amplitude of the input signal and  $L$  is the number of access channels per port. The input-output switch connections are assigned on demand by the control unit (upon availability of input/output ports). A random input/output port assignment process can provide maximum switch throughput.

## REFERENCES

- [1] V. M. DaSilva and E. S. Sousa, "Multicarrier orthogonal CDMA signals for quasi-synchronous communication systems," *IEEE J. Select. Areas Commun.*, vol. 12, no. 5, pp. 842–852, 1994.
- [2] E. A. Sourour and M. Nakagawa, "Performance of orthogonal multicarrier CDMA in a multipath fading channel," *IEEE Trans. Commun.*, vol. 44, no. 3, pp. 356–367, 1996.
- [3] M. Park, K. Ko, H. Yoo, and D. Hong, "Performance analysis of OFDMA uplink systems with symbol timing misalignment," *IEEE Commun. Lett.*, vol. 7, no. 8, pp. 376–378, 2003.
- [4] D. Gerakoulis and G. Efthymoglou, "A multi-carrier multiplexing method for very wide bandwidth transmission," submitted to *EURASIP JWCN*.
- [5] D. Gerakoulis, G. Efthymoglou, F. Koravos, and L. Tassiulas, "A class of multi-carrier CDMA access method for wide-bandwidth wireless channels," to appear in *IEEE PIMRC '05*, Berlin, Germany.
- [6] D. Gerakoulis and E. Geraniotis, *CDMA: Access and Switching: For Terrestrial and Satellite Networks*, chapter 4-5, John Wiley & Sons, Chichester, UK, 2001.
- [7] C. Rose and M. Hluchyj, "The performance of random and optimal scheduling in a time-multiplex switch," *IEEE Trans. Commun.*, vol. 35, no. 8, pp. 813–817, 1987.

**Diakoumis Gerakoulis** received his Ph.D. degree from the City University of New York in 1984, his M.S. degree from the Polytechnic Institute of New York in 1978, and his B.S. degree from New York Institute of Technology in 1976; all in electrical engineering. From 1984 to 1987 he was an Assistant Professor in the Electrical Engineering Department at Pratt Institute, Brooklyn, New York and, from 1987 to 1989, an Associate Professor in the Center of Excellence in Information Systems at Tennessee State University. In 1989 he joined AT&T Bell Laboratories as a member of technical staff, where he worked on common channel signaling and radio access technologies for personal communications. In 1996 he joined AT&T Laboratories where he was involved in the system design, analysis, and performance of common air interfaces for PCS. In 1998 he joined AT&T Labs-Research as a Principal Member of technical staff where he was involved in wideband access technologies for wireless and digital subscriber lines. In 2004 he joined General Dynamics Advanced Information Systems where he is currently a Senior Lead Engineer in systems and he is involved in ad hoc and sensor networks. He holds eight US patents and he is the coauthor of the book *CDMA: Access and Switching*, John Wiley, February 2001. He has also published many papers in journals and conference proceedings in the areas of satellite switching and multiple access, spread-spectrum access and synchronization, and multicarrier CDMA for wireless communications.

